Derivatization of 4-(Dimethylamino)benzamide to Dual Fluorescent Ionophores: Divergent Spectroscopic Effects Dependent on N or O Amide Chelation

by **Jean-Pierre Malval** and **René Lapouyade***

Laboratoire d'Analyse Chimique par Reconnaissance Moléculaire (LACReM), Ecole Nationale Supérieure de Chimie et de Physique de Bordeaux (ENSCPB), F-33607 Pessac Cedex
(Phone: ++33 5 56 84 62 70; e-mail: lapouyad@enscpb.u-bordeaux.fr)

Dedicated to Professor *André M. Braun* on the occasion of his 60th birthday

Starting from the pentafluorophenyl ester of 4-(dimethylamino)benzoic acid, two dual fluorescent amide ligands with aza-15-crown-5 and 2-(aminomethyl)pyridine were obtained for sensing, respectively, alkali (alkaline-earth) and transition (heavy) metal cations. The crystal structure of the copper(II) complex is reported. The Cu^{2+} is coordinated through the pyridine N- and amide O-atoms of two symmetry-related ligands. The azacrown-directed Ca-chelation to the N-atom of the amide leads to a slight quenching of the two fluorescence bands. In contrast, the pyridine directed Cu^{II}-chelation to the O-atom of the amide enhances the short-wavelength emission 17-fold over the locally excited state (LE), quenching the twisted intramolecular charge-transfer (TICT) emission, and, as a result, the intensity ratio I(LE)/I(TICT) provides an accurate and sensitive measurement of the Cu^{II} concentration. These different cation effects are dependent on which atom (N *vs.* O) of the amide function participates in cation coordination: while the Ca^{2+} interaction with the N-atom electron pair leads to the deconjugation of the amide N-atom from the fluorophore, Cu^{2+} interaction with the lone pair of the O-atom of the carbonyl group increases the energy of the n-π^* but also of the ^1L_a transition and therefore close the channel to the TICT state.

1. Introduction. – The detection of ions in various media by fluorometry, a very sensitive and nondestructive analytical method, is often realized with fluorescent sensors [1]. Generally, fluoroionophores are modular systems where the ionophore is either attached to the fluorophore through an isolating chain or is an integral part of the π-electron system [2]. While, in the former case, ion complexation produces a change in fluorescence intensity, for the later system, both spectral and intensity changes of the fluorophore emission occur, allowing measurement of the recognized species from the intensity ratio at two emission wavelengths with opposite ion-sensitivity responses [3]. These intrinsic probes are usually designed as donor-acceptor substituted π-conjugated systems. In most cases, the ionophore is the electron-donor substituent of the fluorophore and coordination of a cation leads to a pronounced blue shift of the intramolecular charge transfer (ICT) absorption band [4] but often to only small changes in fluorescence because of the decoordination of the cation from the fluorophore excited state [5–7]. When the excited state of the probes is weakly polar, a new emission band, a mirror-image of the absorbance of the complex, appears [8]. There are a few examples where the cation interacts with the electron-acceptor group of the fluorophore. As a result the ICT process is increased and there is a red shift in the absorbance and sometimes a higher fluorescence quantum yield results [9]. Even from electronically symmetrical probes, a cation directing and enhancing the ICT process in

the excited state of the chromophore with a red-shifted emission has been reported [10]. Dual emitting fluorophores, which fluoresce from two excited states of very different charge-transfer character provide an unique opportunity to sense the influence of cation binding on the ICT transition.

Precisely, we showed that 4-(dimethylamino)benzonitrile (DMABN) with two fluorescing excited states, the locally excited (LE) state and the twisted intramolecular charge transfer (TICT) state, of considerably different charge-transfer character [11], could be derivatized to 4-azacrowns benzonitrile, (DMABN-crown), a fluoroionophore that signals the presence of Ca^{2+} by an increase in the relative intensity of the emission band from the less-polar excited state [12]. *Collins et al.* described 4-(1,4,8,11-tetraazacyclotetradec-1-yl) benzonitrile (DMABN-cyclam), which, in addition to the fluorescence of the LE and TICT states, leads to an intramolecular exciplex fluorescence, and uniquely responded to the addition of micromolar quantities of transition-metal cations with varying changes in the triple fluorescence emission [13]. We report now the derivatization of the acceptor part of 4-(dimethylamino)benzamide (DMABA), a compound that also gives two fluorescence bands [14], into two classes of fluoroionophores: *i*) when the N-atom of the amide is part of a monoaza-15-crown-5, the corresponding DMABA-crown5 should be a dual fluorescent sensor for s-block alkali and alkaline-earth metal cations interacting with the fluorophore through the N-atom of the amide function (Class A); *ii*) when the N-atom of the amide bears an *o*-methylenepyridine group (DMABA-MP), transition metal ions, particularly Cu^{II} cations, which have a high thermodynamic affinity for typical N,O-chelate ligands [15], should be bound by the N-atom of the pyridine and the O-atom of the amide group (Class B).

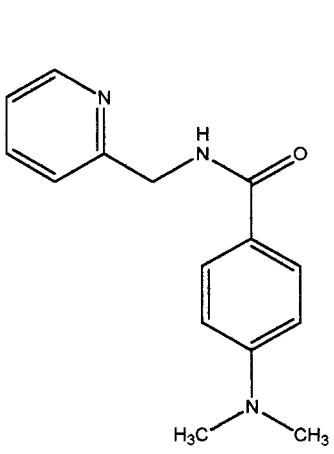

DMABA-MP

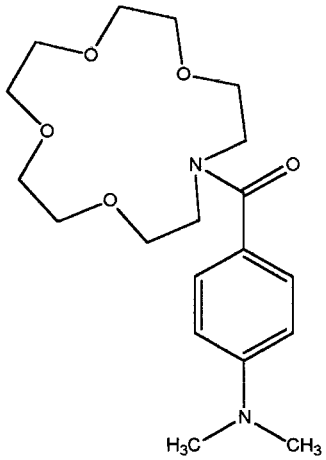

DMABA-Crown5

If the coordination of cations by these two models of molecular probes leads to different spectroscopic effects (absorbance or/and emission), they should provide useful optical characteristics for a sensitive test of the cations coordination sites of the widespread amide derivatives.

2. Results. – DMABA-Crown5 and DMABA-MP have been easily obtained from the pentafluorothiophenyl ester of 4-(dimethylamino)benzoic acid [16], as a common intermediate, by reaction with monoaza-15-crown-5 and 2-(aminomethyl)pyridine, respectively.

Excited-State Polarity of the Two Probes. The absorbance spectra were found to be rather insensitive to the increase of solvent polarity. From a previous study of DMABA and the *N*,*N*-dimethyl and *N*,*N*-diethyl derivatives [14], we can assign the distinctive shoulder around 300 nm, in nonpolar solvents, to the ^1L_b-type transition and the stronger band at 280 nm to ^1L_a-type transition which shifts to the red in polar solvents (*Fig. 1*,*a*).

In relation to the first excited-state inversion, the fluorescence spectra of DMABA-Crown5 and DMABA-MP show a considerable evolution from a single emission in hexane to a major TICT emission in MeCN (*Table 1* and *Fig. 1, b*). This is the result of a higher dipole moment in the relaxed fluorescing state compared to the ground state. If we assume that the contribution of the change of polarizability $\Delta\alpha_{g-e}$ between ground and excited states is negligible, an estimate of the dipole moment from fluorescence solvatochromism can be obtained by the *Lippert-Mataga* equation [17][18]

$$\nu_{fluo} = -2\,\mu_c\,(\mu_e - \mu_g)\,\Delta f'/hc\varrho^3 + \text{const.} \quad (1)$$

where h is *Planck*'s constant, c the speed of light, ν_{fluo} the fluorescence maximum in a solvent of dielectric constant ε and refractive index n, and $\Delta f' = [(\varepsilon-1)/(2\varepsilon+1)] - 0.5\,[(n^2-1)(2n^2+1)]$ is the solvent polarity parameter. The slope of a plot of ν_{fluo} *vs.* $\Delta f'$ gives the value of $\mu_e(\mu_e - \mu_g)/\rho^3$. This allows estimation of the excited-state dipole moment (μ_e) from the solvent cavity (*Onsager*) radius (ρ) and the ground-state dipole moment (μ_g), provided that the dipole-moment direction does not change from ground to excited states.

Table 1. *UV Absorption Maxima* (λ_{abs}), *Fluorescence Emission Maxima* (λ_{fl}), *and Fluorescence Quantum Yields* (ϕ_{fl}) *of DMABA-Crown 5 and DMABA-MP*

Compound	Solvent[a])	λ_{abs} [nm]	λ_{fl}[nm] LE	TICT	ϕ_{fl} LE	TICT
DMABA-Crown5	Hexane	276	334	–	0.020	–
	Bu_2O	278	343	–	0.010	–
	Et_2O	279	346	390	0.004	0.004
	THF	280	350	421	0.005	0.006
	MeCN	282	359	484	0.002	0.008
DMABA-MP	Hexane	284	332	–	0.009	–
	Et_2O	291	342	366	0.007	0.005
	THF	297	351	455	0.023	0.072
	MeCN	298	359	474	0.001	0.006

The structures of the two probes have been drawn with HyperChem and optimized with the AM1 method. The radius (ρ) of the equivalent sphere for the molecular volume of the fluorophore is estimated to be 0.5 nm, and, from the ZINDO/S method, we calculated the dipole moments in the ground state, $\mu_g = 3.6$D. With these values, the slope of ν_{fluo} *vs.* $\Delta f'$ leads to the dipole moments in the excited states: for MDABA-

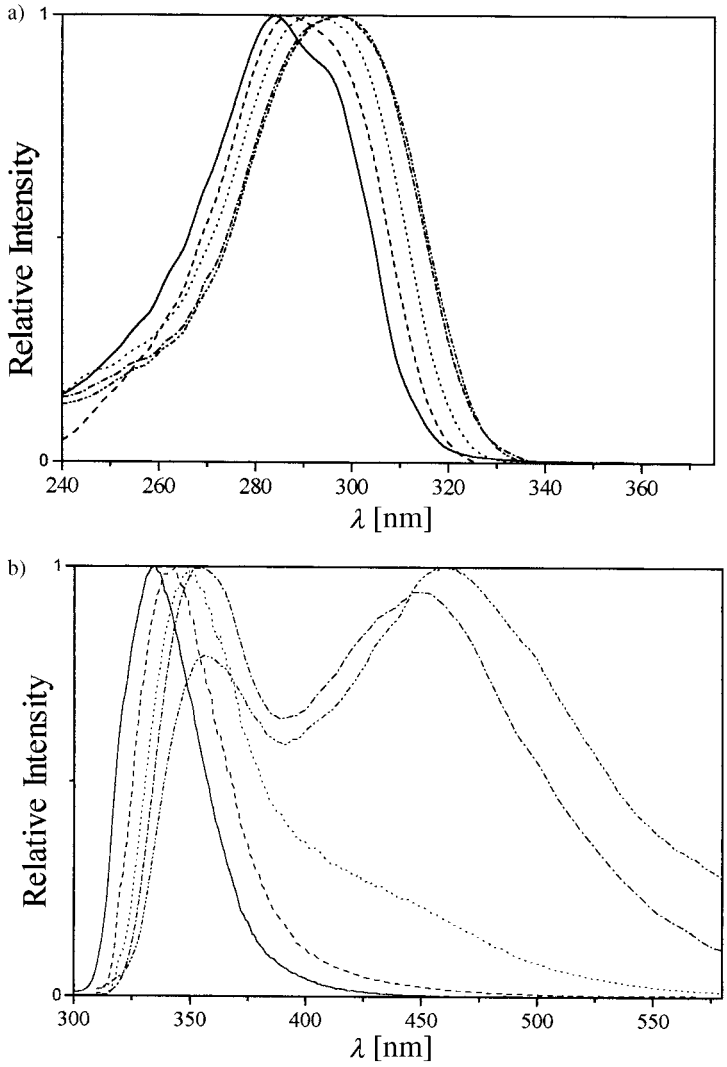

Fig. 1. *Normalized* a) *absorbance and* b) *fluorescence spectra of DMABA-MP in hexane* (—), *Et_2O* (– – – –), *THF* (----), *butyronitrile* (– – – – –), *and MeCN* (– – – – – – –)

Crown5, $\mu_{LE} = 14$D and $\mu_{CT} = 24$D and for DMABA-MP, $\mu_{LE} = 11.3$D and $\mu_{CT} = 20.2$D. This indicates that full CT occurs sequentially *via* relaxation of the LE state to the TICT state, and that the rate constant for this reaction increases with the polarity of the solvent and results in a greater relative intensity of the TICT emission in polar solvents.

Cations-Complexation Effects. The addition of alkali and alkaline-earth metal ions to DMABA-Crown5 in MeCN solution shifts the absorbance maximum to lower energies, as a result of the cation-enhancement of photoinduced charge transfer [9][10][19]. The larger shift is obtained for Ca^{2+} (2820 cm^{-1}) because of its charge

density and the closer size compatibility with aza-15-crown5 (1.98 Å for Ca^{2+}, 1.7–2.2 Å for the estimated diameter of the azacrown5 [20]). The complexation constant derived, according to the treatment described in [9] is $\log K_c = 3.65$ (*Fig. 2,a*).

Surprisingly, the fluorescence spectrum is even less modified upon Ca^{2+} complexation: the two bands are slightly red-shifted, and their relative intensities hardly changed ($I_f(TICT)/I_f(LE) = 4$) in the absence of Ca^{2+}, and this ratio reaches 5 when the

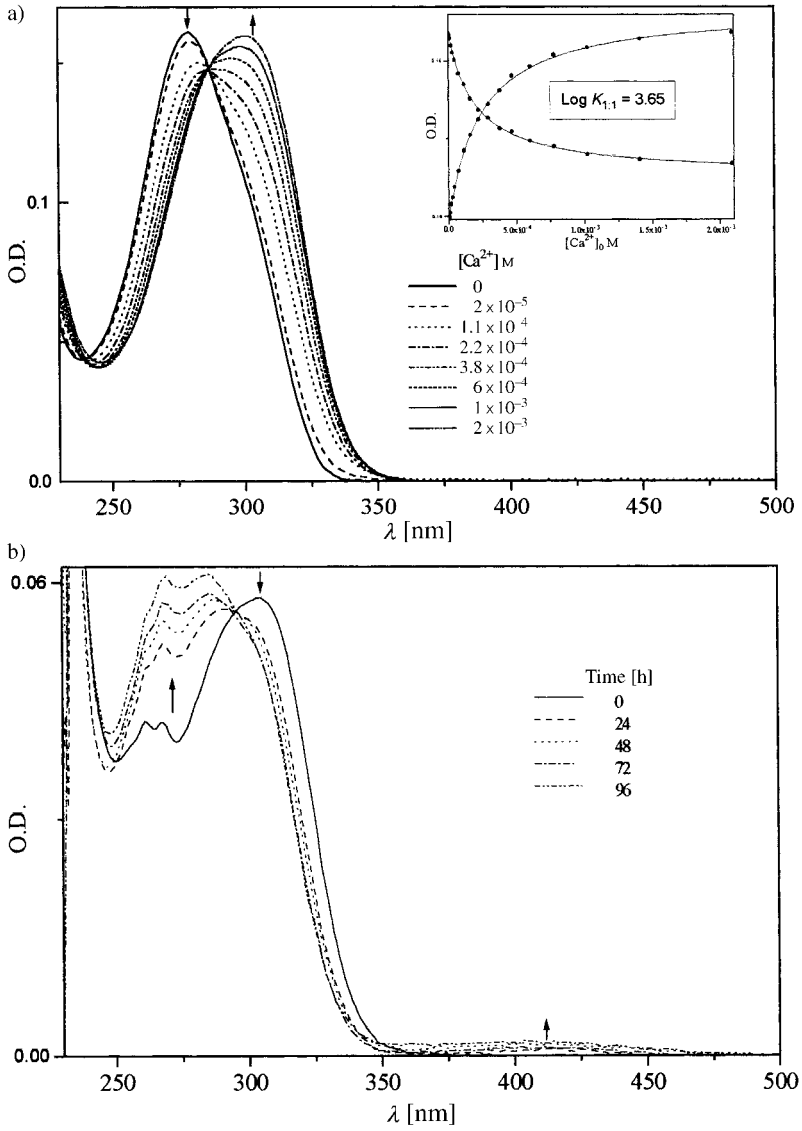

Fig. 2. *Absorbance spectra of* a) *DMABA-Crown5* (1×10^{-5}M) *with increasing concentrations of* Ca^{2+} *in MeCN*, b) *DMABA-MP* (4×10^{-6}M *in MeCN/*H_2O *1:1 with* $Cu(ClO_4)_2$ (3.2×10^{-3}M) *after subtraction of the absorbance corresponding to* $Cu(ClO_4)_2$, *showing the slow complexation*

probe is fully complexed. The fluorescence quantum yield is reduced by half by Ca^{2+} complexation, because the expected increased rate of formation of the TICT state is counterbalanced by its reduced lifetime (from 2.7 ns to 2.2 ns). On the whole, cation complexation by the azacrown leads to a deconjugation of the N-atom of the amide and the complexed probe presents spectroscopic characteristics similar to those of 4-(dimethylamino)benzaldehyde [21].

DMABA-MP was designed for signalling transition metals through ligation to the soft N-atom of pyridine and the O-atom of amide. The later interaction was expected to lower the radiationless transition and, as a result, to enhance the fluorescence yield [14].

We present the spectroscopic properties dependence on pH to define the useful pH range for sensing transition metal cations. In $MeCN/H_2O$ 1:1 solution, the absorbance and fluorescence spectra do not change with the pH in the range 5–14. At lower pH, protonation of the N-atom of the pyridine ring ($pK_a = 3.6$) leads to a small red-shift in the absorbance (λ_{max} shifts from 306 nm to 315 nm) and to an effective quenching of the fluorescence arising from electron transfer to the pyridinium moiety (*Fig. 3*).

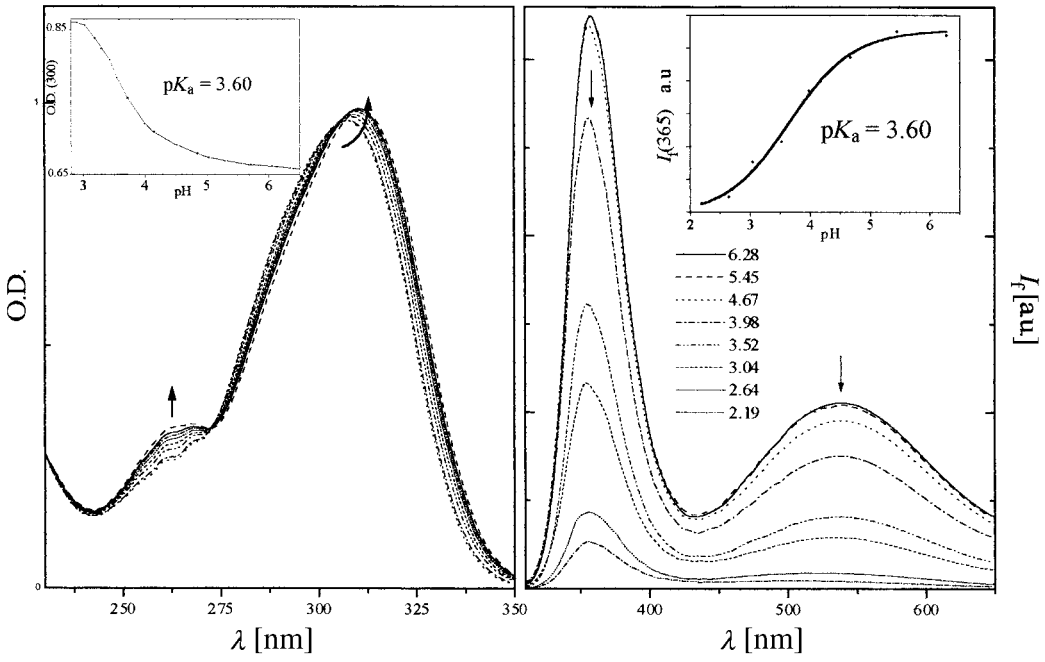

Fig. 3. a) *Absorbance and* b) *fluorescence spectra of DMABA-MP in MeCN/H_2O 1:1 as a function of pH.* Insets: pK_a determination from *a*) absorbance at $\lambda = 300$ nm and *b*) fluorescence at $\lambda = 365$ nm.

At neutral pH, several cations (Zn^{2+}, Co^{2+}, Ni^{2+}, *etc.*) were added without marked changes in the absorbance spectrum, but, with Cu^{2+}, there is a clear blue shift of the ^1L_a-type transition absorbance and appearance of the weak metal-centered transition at longer wavelengths (*Fig. 2,b*). The absorbance spectrum becomes stable after 70 h, at room temperature. Similarly, the fluorescence spectra were not significantly altered by

the different transition metal cations, except with Cu^{2+}, which led to a pronounced increase in the first band (17-fold) and disappearance of the TICT emission (*Fig. 4*). The change of the fluorescence intensity upon Cu^{2+} addition, is time dependent, and an approximately constant signal is obtained after 70 h (*Fig. 4*, *Inset a*). This time evolution reveals a slow complexation, not a chemical reaction because this process is reversible: dilution of the cation with aliquots of the probe solution restored the initial emission.

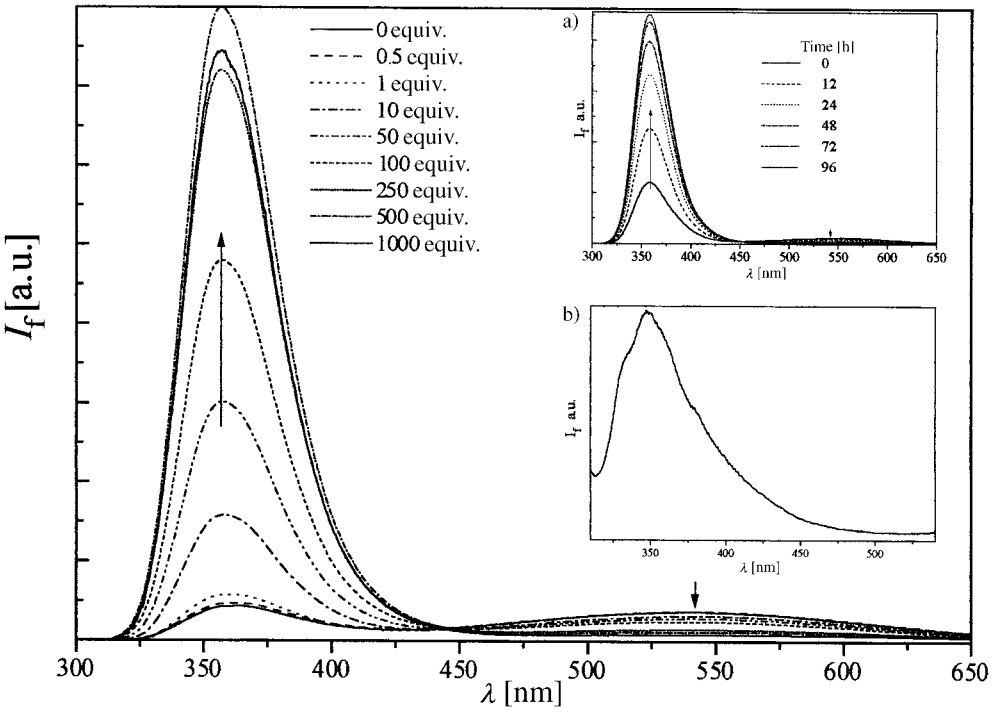

Fig. 4. *Fluorescence spectra of DMABA-MP* (4×10^{-6} M) *in MeCN/H_2O 1:1 with different concentrations of $Cu(ClO_4)_2$* (Insets: *a*) DMABA-MP+10 equiv. of Cu^{II}, time-dependent fluorescence enhancement; *b*) front-face fluorescence from crystals of $(DMABA\text{-}MP)_2 \cdot Cu(ClO_4)_2 \cdot 3H_2O$.

Analysis according to [9] of the evolution of the fluorescence spectra as a function of the cation concentration, at equilibrium (*Fig. 4*) reveals the formation of a complex with two ligands for Cu^{2+}. The apparent association constant for this 1:2 stoichiometry is $\log K_{21} = 8.3 \pm 0.2$.

This is the first example of cation coordination on the acceptor side of a D-A chromophore leading to reduced charge transfer in the excited state. This property is perhaps useful as a probe for Cu^{2+} because of the enhanced fluorescence, particularly of the ratio I(LE)/I(TICT), although the slow complexation precludes rapid analysis.

Structural Analysis of Cu^{2+}-Complexed DMABA-MP. To ascertain the coordination sphere of Cu^{2+} with DMABA-MP, we performed an X-ray crystal-structure analysis, shown in *Fig. 5*.

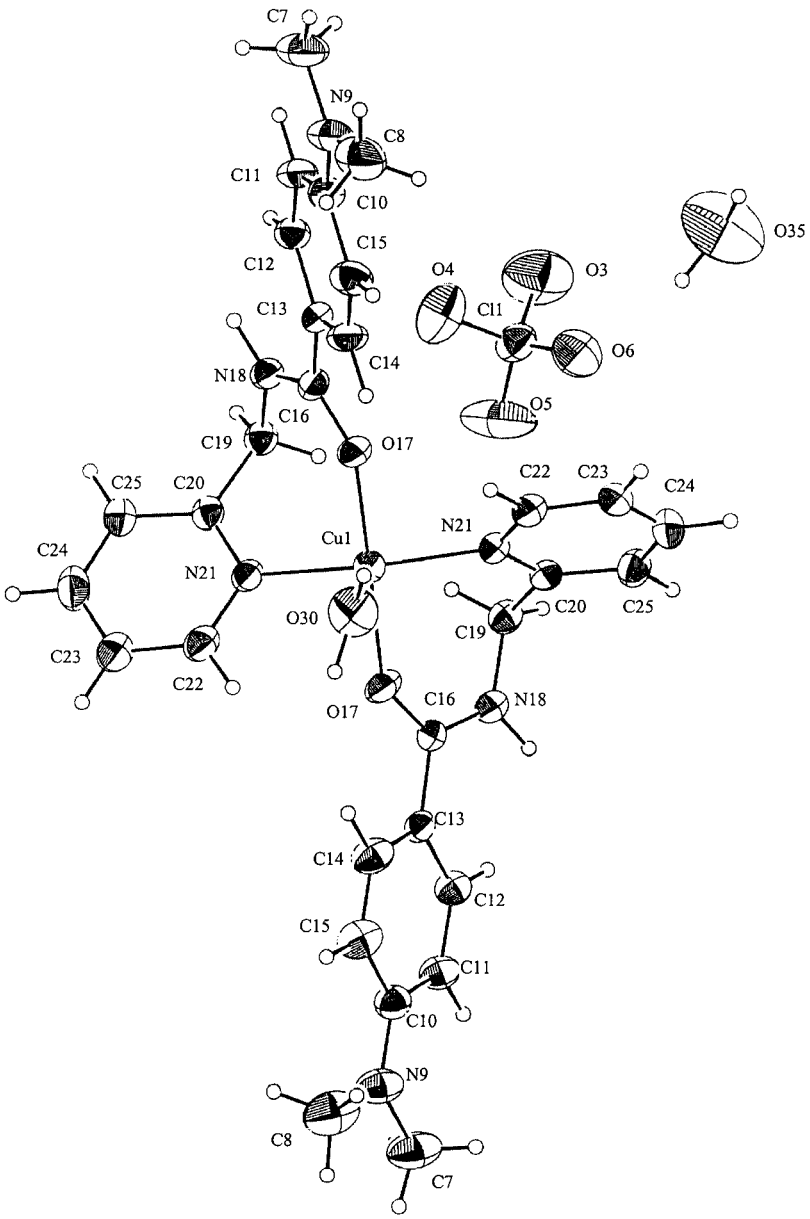

Fig. 5. *X-Ray structure of (DMABA-MP)$_2$·Cu(ClO$_4$)$_2$·3 H$_2$O*

The cation Cu^{2+} is bound to the ligand by the pyridine N(21) and the carbonyl O(17) atoms, forming two short bonds of, respectively, 1.992(4) Å and 1.951(4) Å with a bite angle of 92.5(2) Å (*Table 3*). The two ligands are in the pseudo-equatorial square plane of the complex while a H_2O molecule is located in the axial position, Cu–O(3)

(2.998(4) Å). This cation is counterbalanced by two perchlorate anions. This conformation is essential for the fluorescent properties.

At the electron-donor side, the inversion angle θ between the plane through the three atoms C(7), N(9), and C(8) of the dimethylamino group and that of the phenyl ring amounts to 0.9(1)° typical for a completely planar sp^2 N-atom. The sum of the angles around the amino N-atom N(9) being 360° is also in agreement with a planar sp^2 N-atom. It is noteworthy that DMABN, which is the archetype of related dual fluorescent fluorophores, presents some pyramidalization of this N-atom ($\theta = 10.8°$)

Table 2. *Crystallographic Data, Data Collection, and Refinement Parameters for (DMABA-MP)$_2$·(CuClO$_4$)$_2$ ·3 H$_2$O*

Chemical formula	$(C_{15}H_{17}N_3O)_2 \cdot Cu(ClO_4)_2 \cdot 3H_2O$
Formula weight	827.1
Crystal system	Monoclinic
Space group	*C*2/c
Z	4
Cell parameters	
a, *b*, *c* [Å]	16.5384(5), 16.4926(4), 16.0260(4)
β [°]	120.56(2)
V [Å^3]	3764(2)
d [g cm^{-3}]	1.460
μ (mm^{-1})	0.818
Data collection	
Device	*Kappa*-CCD
T (K)	298
Reflections collected	4469
Observed data [$I > 3\sigma(I)$]	2700
R, *wR*, *S*	0.058, 0.086, 1.89

Table 3. *Selected Bond Lengths* [Å], *Bond Angles* [°], *and Dihedral Angles* [°] *of (DMABA-MP)$_2$ · Cu(ClO$_4$)$_2$ · 3H$_2$O* (compared to reference bond lengths, see text)

		CSD[a])
N(21)–Cu(1)	1.992(4)	
O(17)–Cu(1)	1.951(4)	
O(30)–Cu(1)	2.998(4)	
C(16)–O(17)	1.258(5)	1.23(1)
C(16)–N(18)	1.311(5)	1.34(2)
C(13)–C(16)	1.456(5)	1.50(1)
O(17)–Cu(1)–N(21)	92.5(2)	
O(17)–Cu(1)–O(30)	86.0(1)	
C(16)–O(17)–Cu(1)	154.7(9)	
C(11)–C(10)–N(9)–C(8)	179.3(5)	
C(12)–C(13)–C(16)–O(17)	164.0(4)	
C(14)–C(13)–C(16)–N(18)	163.6(4)	
C(13)–C(16)–N(18)–C(19)	179.5(0)	
C(16)–N(18)–C(19)–C(20)	72.9(4)	
C(19)–C(20)–N(21)–C(22)	179.8(0)	

[a]) From *Cambridge Structural Database*, bond lengths of uncoordinated, structurally similar amides.

[22] while the twist angle φ, defined as the angle between the α C-atoms of the amine substituents and the Ph mean plane, amounts only to 0.5° [23].

We compared bond lengths of the electron-acceptor substituent coordinated to Cu^{2+}, with an analysis of the *Cambridge Structural Database* (CDS) of structures containing a Ph attached to the carbonyl of an amide, and the N-atom was substituted with a sp^3 C-atom (*N*-methylbenzamide model) [24]. The coordination of Cu^{2+} leads to a lengthening of the C=O bond (1.258 *vs.* 1.23 Å), a shortening of the C–N bond (1.31 *vs.* 1.34 Å) and of the C(13)–C(16) bond (1.456 *vs.* 1.50 Å), and the torsion angle between the planes of the benzene and the amide group ring (16°) is in the lower limit of the 11–33° range statistically observed. These effects compare well with the changes observed in the amide bond lengths upon metal coordination; specifically, an increase in the carbonyl C–O bond of 0.03 Å and a decrease in the carbonyl C-atom to N-atom bond length of 0.025 Å [25].

The fluorescence spectra of the complex in the solid state (*Fig. 5*, *Inset b*) shows only one band at the same wavelength as in solution, giving a strong support for a single structure regardless of the phase.

3. Discussion. – Molecules containing the amide functionality are potentially useful in a variety of applications, including as complexing agents for the selective extraction of f-elements and of precious metals, and as improved ligands for magnetic resonance imaging agents. In a recent review [25] the results of a systematic search of the *Cambridge Structural Database* (CSD) have been analyzed to help define the structural features of metal-amide coordination chemistry. Various experimental techniques were used to examine amide metal interactions in these bidentate ligands but, while the multiple fluorescence of benzanilide was thoroughly investigated [26], we are not aware of any fluorescence study of aromatic amides in relation to a regiospecific molecular recognition of the amide function. Nevertheless, secondary amides are used as anion-selective receptors for optical/electrochemical sensing, through H-bonding [27]. The amide group is also used as a linker and serves as a conformational control element in the construction of diad and triad molecules designed for photoinduced electron transfer.

Electron transfer between a TICT state and electron donors or acceptors have been reported [28]. For the quenching by electron acceptors, one can consider that only the radical anion part is involved. Comparison of the reduction potentials of benzamide (−2.2 V) [29], which models the acceptor part of DMABA-BP in the TICT state, pyridine (−2.62 V) [30], and of the pyridinium group (−1.54 V) [31] (all *vs.* SCE) shows that, only for the protonated pyridine, is the condition of exothermicity for TICT quenching by electron transfer fulfilled.

Recently, *Effenberger* and co-workers reported a similar photoinduced intramolecular charge separation between the anthryl and *N*-methylpyridinium moieties [32].

Regarding the different photophysical effects observed with the two probes, they are obviously the result of regiospecific coordination of the metal cations.

With s-block alkali and alkaline-earth metal cations, the interaction with the N-atom of the electron-accepting substituent leads to a red shift of the absorption. It is the result of the cation-induced enhancement of the electron-withdrawing character of the

carbonyl group through deconjugation of the N-atom. The electronic effect of the N-chelated amide group becomes that of a ketone. We observed a small red-shift and a decrease of the fluorescence yield of DMABA-Crown5 because the N-chelation not only increases the charge-transfer character of the first π-π^* transition, but also lowers the energy of the n-π^* transition and accordingly increases the nonradiative deactivation with the result of a lowering the quantum yield of fluorescence.

Generally, the binding of a transition metal with an incomplete d level ($3d^n$, $n < 10$) causes quenching of the fluorescence emission of the probe through two possible mechanisms: electron transfer or energy transfer. Both mechanisms have been observed with Cu^{2+} ($n = 9$). With regard to electron transfer, oxidative quenching of an anthracene-substituted fluorophore with Cu^{2+} has been observed with S-donor ligands that stabilize Cu^{1+} [33], while amidate multidentate ligands that interact strongly with Cu^{3+} have resulted in reductive quenching of the same fluorophore [34]. For dansyl sulphonamides, the quenching rate constant remains high at 77 K, suggesting at least a contribution from the energy-transfer mechanism [35].

Sensors in which the binding of Cu^{2+} causes an increase in the fluorescence emission are very rare. We are aware of a trianthrylcryptand reported by *Bharadwaj* and co-workers, where the absence of quenching is assigned to the cryptate effect [36]. The redox activity of the metal ion is suppressed, as donor atom rearrangement upon oxidation/reduction is energetically unfavorable. Another example was reported by *Rurack et al.* [37] with fluoroionophores, where the receptor units are less efficient quenchers of the fluorophore when they are complexed with Hg^{2+}, Ag^{+} or Cu^{2+}.

With DMABA-MP, the fluorescence enhancement observed upon copper(II) binding does not belong to any of these mechanisms. As the low quantum yield of fluorescence of these amides has been assigned to a nonradiative channel through the n-π^* states [14], we propose that the copper coordination to the carbonyl raises the energy of this state with the result of a slowing down of the nonradiative transitions. Actually, copper coordination not only increases the yield of fluorescence, but, more precisely, it is the first LE state, the less polar one, that becomes highly emitting and does not lead anymore to the TICT state. The absorbance spectrum of the Cu^{II} complex is shifted to the blue. This means that the interaction of Cu^{2+} with the carbonyl group decreases the acceptor strength of the amide group, in contrast with the effect of alkali and alkaline-earth metal cations in coordination in esters. This can be tentatively rationalized by an increased contribution of the charge-separated resonance form involving the N-atom of the amide group as donor upon cation coordination (shorter C–N bond). When this contribution is negligible (ester *vs.* amide) the spectroscopic results are opposite. Thus alkali and alkaline-earth metal cations interacting with oxygen atom of the carbonyl group of esters lead to a red-shift of the absorption and a huge increase of the fluorescence quantum yield assigned to an increase of the electron accepting character of the carbonyl group and of the n-π^* state energy respectively [19].

4. Conclusion. – We have shown that electronic absorbance and emission of substituted benzamides provide sensitive techniques to identify which atoms in the amide function are bound to the metal ion. Moreover, we have obtained a selective Cu^{2+} sensor in $MeCN/H_2O$ mixtures with large fluorescence enhancements (17-fold for

mmolar cation), which allow measurements of the Cu^{2+} concentration from relative fluorescence intensity at two wavelengths with intensity ratio change from 1 (without cupric cation) to *ca.* 100 with mmolar concentration of Cu^{II}.

We thank Dr. *M. Cotrait* for the crystallographic data and Dr. *J.-P. Desvergne* for lifetime measurements.

Experimental Part

General. UV/VIS Absorbance spectra: *Perkin-Elmer Lambda 2* spectrometer. Corrected stationary fluorescence spectra: *Hitachi F-4500* spectrofluorimeter; fluorescence quantum yields were determined by comparison with quinine sulfate in 0.1N H_2SO_4 ($\phi_f = 0.52$). Fluorescence lifetimes were obtained by the time correlated single photon counting technique (*Applied Photophysics*) and mathematical deconvolution [38]. IR: ν in cm^{-1}. ^1H- and ^{13}C-NMR Spectra: *Bruker* instrument; δ in ppm, J in Hz. MS: in m/z (%).

X-Ray crystallography was tiny, prismatic, colorless crystals grown from a soln. of DMABA-MP in MeCN/H_2O. All data were collected at 298 K with a *Kappa-CCD* device with Mo-K_α radiation (0.7107 Å). Complete data sets were collected to a maximum θ limit of 27°. The structure was solved by direct methods with SIR92. The lattice constants are listed with other relevant crystal data in *Table 2* and selected bond lengths (Å), angles (°), and dihedral angles (°) are reported in *Table 3*.

Materials. DMABA-Crown5. Pentafluorothiophenol (2.4 g, 12 mmol) and dicyclohexyl carbodiimide (DCC) (2.5 g, 12 mmol) were added to a stirred suspension of 4-(dimethylamino)benzoic acid (1.65 g, 10 mmol) in 20 ml of anhydrous $MeCl_2$ at 0°. The mixture was left stirring at 0° for 1 h and at r.t. for 14 h. Precipitated dicyclohexylurea was removed by filtration and the filtrate was passed through a silica-gel column, eluting with $MeCl_2$. Evaporation of the solvent gave the ester (3.3 g, 95%). Light yellow oil. ^1H-NMR (250 MHz, $CDCl_3$): 3.07 (*s*, 6 H, Me_2-N); 6.63 (*d*, 2 H); 7.86 (*d*, 2 H).

Part of this oil (1.83 g, 5 mmol) was dissolved in $MeCl_2$ (15 ml) and a soln. of aza-5-crown-15 (1.095 g, 5 mmol) and Et_3N (0.505 g, 5 mmol) in $MeCl_2$ (5 ml) was added. After stirring for 16 h, the solvent was evaporated and a soln. in $MeCl_2$ of the crude product was passed through silica gel, eluting with $MeCl_2$ followed by $MeCl_2$/MeOH 9:1. Evaporation of the eluent gave the amide (0.82 g, 45%), which became solid upon refrigeration. IR (KBr): 2900, 1625, 1510, 1450, 1350, 1200, 1125. ^1H-NMR (250 MHz, $CDCl_3$): 2.91 (*s*, Me_2N); 3.59 (*m*, 16 H, CH_2O); 3.71 (*t*, 4 H, CH_2N); 6.59 (*d*, 2 arom. H, $^2J_{ax} = 8.84$); 7.28 (*d*, 2 arom. H, $^2J_{a'x'} = 8.83$). ^{13}C-NMR ($CDCl_3$, 250 MHz): 40.27 (MeN); 69.83 (CH_2-N); 70.33 (CH_2O); 71.13 (CH_2O); 111.32 (arom. C, *o* to Me_2N); 123.64 (arom. C−C=O); 128.64 (arom. C, *o* to C=O); 151.25 (arom. C−NMe_2); 172.89 (C=O). MS: 366 (2, $M^{\bullet+}$), 148 (100, [M − azacrown]$^+$).

DMABA-MP. A soln. of 2-(aminomethyl)pyridine (0.648 g, 6 mmol) and Et_3N (0.6 g, 6 mmol) in $MeCl_2$ (5 ml) was added to a stirred soln. of the pentafluorophenyl ester of 4-(dimethylamino)benzoic acid (1.83 g, 5 mmol) in $MeCl_2$ (15 ml). After stirring for 16 h, the solvent was evaporated and a soln. of the residue in $MeCl_2$ was passed through a plug of silica gel, eluting successively with $MeCl_2$ and $MeCl_2$/MeOH 9:1. Evaporation of the eluent followed by crystallization from MeOH gave the amide as a white solid (0.79 g, 62%). ^1H-NMR (200 MHz, $CDCl_3$): 3.02 (*s*, 6 H); 4.75 (*d*, 1 H, $J = 4.92$); 6.68 (*d*, 2 H, $J = 9.1$); 7.17–7.45 (br. *m*, NH, 2 H of Pyr); 7.68 (*dt*, 1 H, Pyr); 7.79 (*d*, 2 H, $J = 9.1$); 8.56 (1 H, *o* to Pyr). MS: 255 (41, $M^{\bullet+}$), 148 (100, [M − 2-(aminomethyl)pyridine]$^+$), 107 (28).

REFERENCES

[1] 'Chemosensors of Ion and Molecule Recognition', Ed. J.-P. Desvergne, A. W. Czarnik, NATO Series C 492, Kluwer, Dordrecht, 1997.
[2] A. P. de Silva, H. Q. N. Gunaratne, T. Gunnlaugsson, A. J. M. Huxley, C. P. McCoy, J. T. Rademacher, T. E. Rice, *Chem. Rev.* **1997**, *97*, 1515.
[3] B. Valeur, in 'Probe Design and Chemical Sensing', Ed. J. R. Lakowicz, Plenum, New York, 1994, p. 21; W. Rettig, R. Lapouyade, in 'Probe Design and Chemical Sensing', Ed. J. R. Lakowicz, Plenum, New York, 1994, p. 109–149.
[4] H.-G. Löhr, F. Vögtle, *Acc. Chem. Res.* **1985**, *18*, 65.
[5] J. Bourson, B. Valeur, *J. Phys. Chem.* **1989**, *93*, 3871.
[6] R. Mathevet, G. Jonusauskas, C. Rullière, J.-F. Létard, R. Lapouyade, *J. Phys. Chem.* **1995**, *99*, 15709.

[7] M. M. Martin, P. Plaza, Y. H. Meyer, F. Badaoui, J. Bourson, J.-P. Lefèvre, B. Valeur, *J. Phys. Chem.* **1996**, *100*, 6879.
[8] P. Crochet, J.-P. Malval, R. Lapouyade, *Chem. Commun.* **2000**, 289.
[9] J. Bourson, J. Pouget, B. Valeur, *J. Phys. Chem.* **1993**, *97*, 4552.
[10] S. Delmond, J.-F. Létard, R. Lapouyade, R. Mathevet, G. Jonusauskas, C. Rullière, *New J. Chem.* **1996**, *20*, 861.
[11] W. Rettig, *Angew. Chem., Int. Ed.* **1986**, *25*, 971.
[12] J.-F. Létard, S. Delmond, R. Lapouyade, D. Braun, W. Rettig, M. Kreissler, *Rec. Trav. Chim. Pays-Bas* **1995**, *114*, 517.
[13] G. E. Collins, L.-S. Choi, J. H. Callahan, *J. Am. Chem. Soc.* **1998**, *120*, 1474.
[14] D. Braun, W. Rettig, S. Delmond, J.-F. Létard, R. Lapouyade, *J. Phys. Chem.* **1997**, *101*, 6836.
[15] R. Krämer, *Angew. Chem., Int. Ed.* **1998**, *37*, 772.
[16] A. P. Davis, J. J. Walsh, *Tetrahedron Lett.* **1994**, *35*, 4865.
[17] E. Z. Lippert, *Z. Naturforsch.* **1955**, *10a*, 541.
[18] N. Mataga, Y. Kaifu, M. Koizumi, *Bull. Chem. Soc. Jpn.* **1956**, *29*, 465.
[19] I. Leray, F. O. O'Reilly, J.-L. Habib Jiwan, J.-P. Soumillion, B. Valeur, *Chem. Commun.* **1999**, 795.
[20] R. M. Izatt, J. S. Bradshaw, S. A. Nielsen, J. D. Lamb, J. J. Christensen, D. Sen, *Cehm. Rev.* **1985**, *85*, 275.
[21] J. Dobkowski, E. Kirkor-Kaminska, J. Koput, A. Siemiarczuk, *J. Lumin.* **1982**, *27*, 339.
[22] A. Heine, R. Herbst-Irmer, D. Stalke, *Acta Crystallogr., Sect. B*, **1994**, *50*, 363.
[23] A. Gourdon, J.-P. Launay, M. Bujoli-Doeuff, F. Heisel, J. A. Miehe, E. Amouyal, M.-L. Boillot, *J. Photochem. Photobiol. A: Chem.* **1993**, *71*, 13.
[24] R. Vargas, J. Garza, D. Dixon, B. P. Hay, *J. Phys. Chem. A* **2001**, *105*, 774.
[25] O. Clement, B. M. Rapko, B. P. Hay, *Coord. Chem. Rev.* **1998**, *170*, 203.
[26] F. D. Lewis, T. M. Long, *J. Phys. Chem.* **1998**, *102*, 5327.
[27] P. D. Beer, *Chem. Commun.* **1996**, 689.
[28] L. Habib Jiwan, J.-P. Soumillion, *J. Photochem. Photobiol. A: Chem.* **1992**, *64*, 145; G. Schopf, W. Rettig, J. Bendig, *J. Photochem. Photobiol. A: Chem.* **1994**, *84*, 33.
[29] L. Horner, R.-J. Singer, *Anal. Chem.* **1969**, *723*, 1.
[30] H. Siegerman, in 'Techniques of Chemistry, Vol. V, Part II. Technique of Electroorganic Synthesis', Ed. N. L. Weinberg, Wiley, New York, 1975.
[31] F. Pragst, M. Santrucek, *J. Prakt. Chem.* **1987**, *329*, 67.
[32] T. Hirsch, H. Port, H. C. Wolf, B. Miehlich, F. Effenberger, *J. Phys. Chem.* **1997**, *101*, 4525.
[33] G. De Santis, L. Fabrizzi, M. Lichelli, C. Mangano, D. Sacchi, *Inorg. Chem.* **1995**, *34*, 3581.
[34] L. Fabbrizzi, M. Lichelli, P. Pallavicini, P. Perotti, A. Taglietti, D. Sacchi, *Chem.-Eur. J.* **1996**, *2*, 75.
[35] L. Prodi, F. Bolletta, M. Montaldi, N. Zaccheroni, *Eur. J. Inorg. Chem.* **1999**, 455.
[36] P. Ghosh, P. K. Bharadwaj, S. Mandal, S. Ghosh, *J. Am. Chem. Soc.* **1996**, *118*, 1553.
[37] K. Rurack, M. Kollmannsberger, U. Resch-Genger, J. Daub, *J. Am. Chem. Soc.* **2000**, *122*, 968.
[38] D. V. O'Connor, D. Philips, 'Time Correlated Single Photon Counting', Academic Press, London, 1984.

Received March 14, 2001